

Ameliorative Effects of EUK-134, a Superoxide Dismutase and Catalase Mimetic, in a Rat Model of D-Galactose-Induced Oxidative Stress and Accelerated Aging

Kwang Won Kim^{1,*}, Kwang Song Kim², Kyong Ok Ri³, Hyong Gwan Ri¹, Chung Il Yo², Son Yong Ko², Tok Man Hwang¹

Kwang Won Kim^{1,*}, Kwang Song Kim², Kyong Ok Ri³, Hyong Gwan Ri¹, Chung Il Yo², Son Yong Ko², Tok Man Hwang¹

¹Department of Biochemistry, Faculty of Life Science, Kim Il Sung University, Pyongyang, DEMOCRATIC PEOPLE'S REPUBLIC OF KOREA.

²Graduate School, Kim Il Sung University, Pyongyang, DEMOCRATIC PEOPLE'S REPUBLIC OF KOREA.

³Department of Physiopathology, Pyongyang Medical University, DEMOCRATIC PEOPLE'S REPUBLIC OF KOREA.

*Correspondence

Dr. Kwang Won Kim

Department of Biochemistry, Faculty of Life Science, Kim Il Sung University, Pyongyang, DEMOCRATIC PEOPLE'S REPUBLIC OF KOREA.

Email: kw.kim0708@ryongnamsan.edu.kp

History

- Submission Date: 04-08-2021;
- Review completed: 09-10-2021;
- Accepted Date: 11-11-2021.

DOI : 10.5530/ijcep.2022.9.1.4

Article Available online

<http://www.ijcep.org/v9/i1>

Copyright

© 2022 The Author(s). This is an open-access article distributed under the terms of the Creative Commons Attribution 4.0 International license.

ABSTRACT

Background and Aim: EUK-134, a synthetic superoxide dismutase/catalase mimetic, is a salen-manganese complex that exhibits the catalytic actions of both superoxide dismutase and catalase, important antioxidant enzymes biosynthesized by cells. In the current study, we evaluated the protection effects of EUK-134 against D-galactose-induced oxidative stress and accelerated aging in rats. **Materials and Methods:** D-galactose was sub-cutaneously injected at a dose of 100 mg/kg on the back of rats once daily for 42 days and simultaneously EUK-134 was administered to the rats by intra-abdominal injection at a dose of 5 mg/kg once daily. As a positive control, donepezil was administered to the rats by oral feeding at a dose of 1 mg/kg once daily. Following behavioral tests (eight-arm radial maze test and Morris water maze test), animals were sacrificed on day 42, and their brains were used for histopathological and biochemical assessments of oxidative stress. **Results:** We found that the administration of EUK-134 (5 mg/kg, i.a.) significantly reversed the spatial memory deficits, the brain weight loss, the reduced cerebral cortex thickness, the decreased pyramidal neuron density and the pyramidal layer in brain hippocampus, the decreased superoxide dismutase activity, the decreased catalase activity, the increased malondialdehyde level, the increased acetylcholine esterase activity and the decreased acetylcholine level in the brain hippocampus and prefrontal cortex of D-gal-induced aging rats, as did the administration of donepezil (1 mg/kg, oral). **Conclusion:** These results indicated that EUK-134 possesses neuroprotective effects against D-galactose-induced senescence, probably due to its antioxidant enzyme activities and this shows the availability of EUK-134 in the prevention and treatment of neurodegenerative diseases such as Alzheimer's disease.

Key words: EUK-134, D-galactose, Oxidative stress, Aging, Alzheimer's disease.

INTRODUCTION

Human beings and all living organisms are affected by changes as a consequence of aging which is a gradual and inevitable biological process and complex natural phenomenon of life cycle.^[1] In humans, aging is related by alterations in cellular homeostatic mechanisms leading to diverse health problems such as reduction in hearing and vision, change in body weight, diabetes, hypertension and a range of central nervous disorders.^[2] On the other hand, brain aging, particularly in humans, is characterized by structural changes including gray and white matter volume reductions, modifications in the number and types of neurons and glial cells, and so on.^[3,4] Despite the scientific advances, precise molecular cell mechanisms that affect cellular aging and age-related diseases such as diabetes, cardiovascular disease, cancer, arthritis, osteoporosis, high blood pressure, and Alzheimer's disease are still unknown.^[5]

So far, more than 300 theories with regard to aging were postulated^[6] and one of the first proposed theories of aging is the oxidative stress theory, originally known as the free radical theory, which is known to be one of the most prominent and well studied.^[7] This theory was first proposed by Denham Harman in the mid 1950s and suggests that reactive oxygen species (ROS) from the environment and internal metabolism are a cause of aging. Specifically, it is indicated that ROS affect biomacromolecules such as DNA, lipids and proteins, and are involved in the pathophysiology of many diseases. The term oxidative stress refers to a condition where the levels of ROS significantly overwhelm the capacity of antioxidant defenses in a biological system. Oxidative stress condition can be caused by either increased ROS formation or decreased activity of antioxidants or both in a biological system.^[8] The mitochondrial theory of aging, a theory that extends the core concepts of the oxidative stress theory, was

Cite this article: Kim KW, Kim KS, Ri KO, Ri HG, Yo CI, Ko SY, *et al.* Ameliorative Effects of EUK-134, a Superoxide Dismutase and Catalase Mimetic, in a Rat Model of D-Galactose-Induced Oxidative Stress and Accelerated Aging. Int J Clin Exp Physiol. 2022;9(1):19-27.

proposed by Harman in 1972 and suggests that the basic mechanism of mammalian aging is related to mitochondria dysfunction due to increasing oxidative damage.^[9] The major production site of ROS is the mitochondria.^[10] The mitochondrial theory of aging is based upon a cycle in which somatic mutation of mitochondrial DNA (mtDNA) induces respiratory chain dysfunction, which enhances the production of ROS that damage mtDNA again. Similar to the oxidative stress theory, the resulting accumulation of mtDNA mutations leads to tissue dysfunction and degeneration of tissues, and possibly neurodegenerative diseases. Overall, both theories of aging hypothesize that ROS contribute to the process of aging and are correlated with neurodegenerative disease.

However, despite enormous amount of effort, the mechanism by which oxidative damage causes neuronal death is not well understood. Emerging data from a number of neurodegenerative diseases suggest that there may be common features of toxicity that are related to oxidative damage.^[11,12] A major risk factor for neurodegenerative diseases such as Alzheimer's disease (AD), Parkinson's disease (PD), Huntington's disease, amyotrophic lateral sclerosis and progressive supranuclear palsy is aging.^[13] AD, PD and Huntington's disease are among the most age-related central nervous diseases.^[14] According to the "World Alzheimer Report 2018", 50 million people over the world are suffering with AD, and the AD morbidity is doubling per 20 years.^[15] In the past 30 years, pharmaceutical companies in the world have invested hundreds of billions of dollars in AD drug development, and more than 1000 drugs have been clinically tested. However, there is still no drug discovered to be able to effectively reverse AD. Main reasons include that the pathogenesis of AD is complicated and ambiguous, and AD is a chronic neurodegenerative disease with long pathogenic time.^[16,17]

D-galactose (D-gal) is a chemical substance used for more than twenty years that accelerates aging. Chinese researchers reported in 1999 that injection of a low dose of D-gal into mice could induce changes which resembled accelerated aging, and this aging model showed neurological impairment, shortened animal lifespan, decreased activity of antioxidant enzymes, and diminished immune responses.^[18] Moreover, it has been indicated in specifically affecting spatial memory.^[19,20] Rodent chronically injected with D-gal has been used as an animal aging model to investigate the mechanisms of brain aging and anti-aging therapeutics, because chronic injection of D-gal can cause a progressive deterioration in learning and memory capacity.^[21] In case of accumulation of D-gal in the body, due to its oversupply, D-gal is converted by galactose oxidase to galactitol, an alditol-type sugar alcohol, which in turn lead to the generation of ROS.^[14,22,23] It also increases malondialdehyde (MDA) level and total antioxidant capacity, and decreases the activity of superoxide dismutase (SOD), glutathione peroxidase, monoamine oxidase-B as well as catalase (CAT), all of which increase oxidative stress.^[24,25] In addition, D-gal causes apoptosis (programmed cell death), an important role player in the brain aging. Evidence indicates that both increased oxidative damage and apoptosis may significantly contribute to the development of early cognitive dysfunction in aging.^[26]

SOD and CAT are metalloproteins that catalyze "dismutation" reactions, which detoxify ROS.^[8] The overexpression of these metalloproteins in cell culture and in whole animals has provided protection against the deleterious effects of a wide range of oxidative stress paradigms. The use of SOD and CAT as therapeutic agents to attenuate ROS-induced injury responses has had mixed success.^[27] The principal limitations of clinical using these natural proteins are their large sizes, the consequences of which are low cell permeability, a short circulating half-life, antigenicity and high-manufacturing costs. To overcome many of these limitations, an increasing number of low molecular-weight catalytic antioxidants have been developed.^[28] Among catalytic antioxidants, three manganese-incorporated complexes, namely, EUK-134 (salen mimetic), AEOL-

10150 (*meso*-porphyrin mimetic) and M40403 (macrocyclic mimetic) are already under clinical trials.^[29]

EUK-134, a synthetic SOD/CAT mimetic, is a salen-manganese complex that exhibits the catalytic actions of both SOD and CAT, important antioxidant enzymes biosynthesized by cells.^[30-32] Treatment of wild-type worms with 0.05mM EUK-134 increased their mean life-span by 54 percent, and treatment of prematurely aging worms resulted in normalization of their life-span (a 67 percent increase), suggesting that oxidative stress is a major determinant of life-span and that it can be counteracted by pharmacological intervention in 2000.^[33] However, the research article in 2006 showed that EUK-134 increased lifespan in SOD-deficient flies, but failed to extend the lifespan of normal, wild type animals.^[34]

Recent research results clearly demonstrate that EUK-134 is beneficial in many models of oxidative stress, and in other words possesses protective effects against many diseases and related conditions in which ROS play a causal or contributing role, for example, cardiovascular diseases, metabolic syndrome, neurological diseases, pulmonary diseases, hepatic and gastrointestinal diseases, renal diseases, cancer, and other diseases and conditions. Treatment with EUK-134 prevented respiratory chain abnormalities induced by ionizing radiation in rat astrocyte cultures, suggesting that EUK-134 is an antioxidant that protects the mitochondria.^[35] Peroxynitrite anion (ONOO⁻) scavenger EUK134 markedly ameliorated myocardial ischemia/reperfusion injury.^[36] Pretreatment with mitoprotective antioxidant EUK-134 (10 μM) was effective in the prevention of hypertrophic changes in H9C2 cardiomyocytes, reduction of oxidative stress, and prevention of metabolic shift.^[37] A synthetic SOD/CAT mimetic, EUK-134 and/or a glutathione precursor, N-acetyl cysteine protected polymorphonuclear leukocytes from the toxic effects of zinc and paraquat (a widely used herbicide) in rats.^[38] EUK-134 prevented diaphragm muscle weakness in pulmonary hypertension induced by monocrotaline which was a pyrrolizidine alkaloid extracted from seeds of *Crotalaria spectabilis*.^[39] On the other hand, whole thorax irradiation induced endothelial cell loss in lungs and reduction of superoxide dismutase 1 (SOD1) level. Mesenchymal stem cell therapy protected lungs from radiation-induced endothelial cell loss by restoring SOD1 expression. A similar protective effect was achieved by using the SOD-mimetic EUK-134.^[40] Silencing of an age-inhibiting gene (Klotho) promoted oxidative stress-induced alveolar epithelial cell (AEC) mitochondrial DNA (mtDNA) damage and apoptosis whereas Klotho-enforced expression (EE) and EUK-134, a mitochondrial ROS scavenger, were protective. EUK-134 also played a protective role in the renal circulation in sepsis.^[41] EUK134 protected neuronal cells (human neuroblastoma cell line SK-N-MC) against hydrogen peroxide-induced oxidative stress.^[42] EUK-134 significantly prevented the mitochondrial ROS (superoxide and hydrogen peroxide) increase induced by amyloid β peptide oligomers (AβOs), toxic aggregates with pivotal roles in AD, and thus prevented AβOs-induced mitochondrial dysfunctions.^[43]

However, no experimental data have been proposed that have yet examined the effects of EUK-134 in the accelerated model of aging induced with D-gal. Therefore, the aim of the present study was to evaluate the effects of EUK-134 against D-gal induced oxidative stress, memory impairment and accelerated aging in rats.

MATERIALS AND METHODS

Animals and Treatment

Sprague-Dawley rats (200-250g) were obtained from the Laboratory Animal Center of Pyongyang Medical College. Animals were fed a standard rodent diet and water, and bred in a controlled environment

with 12-hr light-dark cycles. They were treated as recommended in the Guide for the Care and Use of Laboratory Animals issued by the D.P.R.K Association of Laboratory Animal Care. All efforts were made to minimize the number of animals used as well as their suffering.

Sixty-four rats were randomly divided into four groups of 16 animals each and treated for a period of 42 days (six weeks). In the first group (normal group), the distilled water was orally fed, and saline was sub-cutaneously and intra-abdominally injected once daily. In the second group (D-gal group), the distilled water was orally fed, D-gal was sub-cutaneously injected on the back of rats at a dose of 100 mg/kg and saline was intra-abdominally injected once daily. In the third group (D-gal+EUK-134 group), the distilled water was orally fed, D-gal was sub-cutaneously injected at a dose of 100 mg/kg and EUK-134 was intra-abdominally injected at a dose of 5 mg/kg once daily. In the final group (D-gal+DPZ group), donepezil (DPZ) was orally fed at a dose of 1 mg/kg, D-gal was sub-cutaneously injected at a dose of 100 mg/kg and saline was intra-abdominally injected once daily.

Reagents

All chemicals were of the highest available purity grade. Millipore (RO/Syngy) purified water was used for the preparation of reagents.

Preparation of EUK-134

A salen-manganese complex, EUK-134 [manganese 3-methoxy-N,N'-bis(salicylidene)ethylenediamine chloride] is relatively easy to prepare and to purify. It was prepared according to the procedure of Sharpe *et al.*^[44] based on that of Boucher^[45] and Baker *et al.*^[46] The first-step product, salen-H₂ ligand was prepared by the addition of 250 mL of 200 mM ethylenediamine to an equal volume of 400 mM of *o*-vanillin in absolute ethanol. The precipitate was filtered, washed with absolute ethanol and air-dried to give the desired product in 90 % yield. To obtain the second-step product, solid manganese (II) acetate tetrahydrate was added to a stirred suspension of 30 mM salen-H₂ ligand in 95 % ethanol to a final concentration of 30 mM and refluxed for 2 h. The dark-brown solutions were dried under a stream of air. The crude product, a brown solid, was washed with acetone, filtered and air-dried. This acetate complex (salen-Mn acetate, EUK-113) were converted to salen-Mn chloride (EUK-134) through treatment of an aqueous solution (final concentration, 100 mM) of the salen-Mn acetate, warmed to 50°C, with 500 mM KCl dissolved in distilled water. A brown precipitate formed immediately. The suspension was cooled in an ice/water bath and then filtered; the brown solid was washed with water and acetone to give the final product in 70% yield. The concentration of EUK-134 was determined from the absorption spectrum^[45,47] and its elemental analysis, ultraviolet-visible absorbance spectrum, infrared spectrum, SOD activity, catalase activity, peroxidase activity, ¹H NMR spectrum and so on were consistent with the reported structure and the previous data.^[48]

Eight-Arm Radial Maze Test

Behavioral testing using an 8-arm radial maze task was conducted according to the previous method.^[49] The maze apparatus consisted of a central platform (24 cm in diameter) with 8 arms that extended radially. A rat was placed in the platform and allowed to visit each arm to eat 8 pellets in food cups located near the end of each arm. Each test animal was trained once daily to memorize the apparatus. The performance of the test animals in each trial was assessed using two parameters: number of correct choices (defined as choosing arms that had never been visited) and number of incorrect choices (defined as choosing arms that had already been visited). When the test animals made 7 or 8 correct choices and no more than one error in three successive sessions, they

were deemed to have memorized the maze. In other words, the rats had acquired spatial memory of the 8-arm radial maze.

Morris Water Maze Test

The Morris water maze test was performed according to a procedure from the literatures.^[50-52] The test device consisted of a black rounded tank that was 150 cm in diameter and 80 cm in height. Virtually the tank was separated into four identical quadrants: northeast (NE), northwest (NW), southeast (SE) and southwest (SW). A circular platform (15 cm in diameter) was located in the center of the SE quadrant, whose position retained during the experiment. The tank was filled with water until the platform was 2 cm below the water surface and the water temperature was adjusted to room temperature (22±1°C). The experiment included two phases e.g. acquisition training session and the probe trail. Each trial was terminated as soon as the rat had climbed onto the escape platform successfully or when 60s had elapsed. Escape latency is defined as the time taken for the rat to find the hidden platform. In all four animal groups, escape latencies were detected on day 14, 24 and 42.

Histopathological Examination

After the behavioral procedures were completed, rats were euthanized with a mild ether anesthesia and perfused intracardially with 20 mM phosphate-buffered saline (PBS, pH 7.4), for 2 min followed by 10% (w/v) neutral buffered formalin (NBF, pH 7.0) for prefixation of the tissues another 5 min. The brain was dissected out carefully and kept in ice-cold plate immediately according to the previous method.^[53] The excised regions were isolated and washed with normal saline followed by 10% NBF in PBS and stored in 10% NBF overnight at room temperature for postfixation. The tissues were dehydrated in gradient alcohol solutions (30%, 50%, 70%, 80% 90% and 100%). Dehydration was followed by clearing the samples in two changes of xylene (Sulfur free). Samples were then impregnated with two changes of paraffin wax, then embedded and blocked out. The obtained paraffin blocks were then sectioned at 3 μm thickness. The brain sections were de-paraffinized, hydrated, and then stained with hematoxylin-eosin (H-E) for histopathological examination under a light microscope.^[54] Pyramidal neuron density and pyramidal layer thickness in CA1, CA2 and CA3 regions of brain hippocampus of four group rats were determined according to the previous method.^[55]

Biochemical Assays

At the end of the behavioral procedures, the rats were sacrificed on day 42 by decapitation under mild ether anesthesia, and immediately, brains were rinsed with cold saline and weighted. Then the hippocampus and prefrontal cortex were rapidly dissected over ice and tissues were homogenized in cold saline. The homogenates were centrifuged for 30 min at 14 000 rpm at 4°C and the supernatants were separated and kept for the estimation of total protein concentration, SOD activity, CAT activity, MDA level, acetylcholine esterase (AChE) activity and acetylcholine (ACh) level.

The total protein content of homogenates was estimated using the method of Bradford with bovine serum albumin as standard.^[2] SOD activity was estimated from the decreasing rate of nitrite produced by hydroxylamine and superoxide anions, based on an improved nitrite method.^[56,57] CAT activity was estimated according to an improved ammonium molybdate spectrophotometric method^[58] which was based on the reaction of undecomposed hydrogen peroxide with ammonium molybdate to produce a yellowish color. Lipid peroxidation was measured using the thiobarbituric acid (TBA) assay which was based on the reactivity of an end product of lipid peroxidation, MDA with TBA to produce a red adduct.^[59,60]

AchE activity was measured by detecting the absorbance of sym-trinitrobenzene formed in the color reactions between acetylcholine-hydrolyzed choline and acetic acid; choline can react with hydrosulphonyl to generate sym-trinitrobenzene, which is a yellow product. Ach was assayed by detecting the absorbance of a brown product formed in the color reactions between Ach and the substrate of the test kit.^[61-63] All of the procedures completely complied with the manufacturer's instructions.

Statistical Analysis of Data

Results are expressed as mean \pm Standard Error of Mean (SEM) and were analyzed using one-way analysis of variance (ANOVA). Values of $P < 0.05$ were considered significant, and $P < 0.01$ was considered highly statistically significant. The statistical analysis was performed using the GraphPad Prism Software 5.0.

RESULTS

Effect of EUK-134 on the Spatial Memory of D-gal Treated Rats in the Eight-Arm Radial Maze Test

Figure 1 showed that the treatment of rats with D-gal (100 mg/kg, s.c.) significantly decreased the number of correct choices and markedly increased the number of incorrect choices on day 14, 28 and 42, and the longer the injection period was, the smaller the number of correct choice was and the larger the number of incorrect choice was. Meanwhile, the treatment of rats with EUK-134 (5 mg/kg, i.a.) or DPZ (1 mg/kg, oral) both prevented the reduction of the number of correct choices and the increase of the number of incorrect choices (Figure 1). These results suggest that the administration of EUK-134 can significantly improve the spatial working memory ability of D-gal-induced aging rats.

Effect of EUK-134 on the Spatial Memory of D-Gal

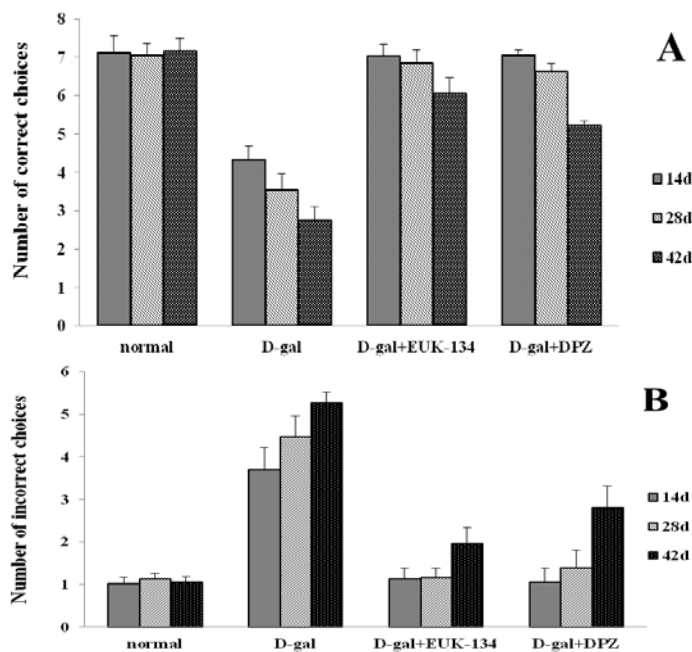


Figure 1: Effect of EUK-134 on (A) the number of correct choices and (B) the number of incorrect choices of rats in the eight-arm radial maze test on different days.

Values are expressed as the mean \pm SEM.

Treated Rats in the Morris Water Maze Test

The average escape latencies in the D-gal group rats were significantly longer than those in the normal group rats. In other words, the treatment of rats with D-gal (100 mg/kg, s.c.) markedly increased the escape latency to the platform on day 14, 28 and 42, and the longer the injection period was, the longer the escape latency was. Meanwhile, the treatment with EUK-134 (5 mg/kg, i.a.) or DPZ (1 mg/kg, oral) both could significantly shorten the escape latencies of D-gal-induced aging rats (Figure 2). These results suggest that the administration of EUK-134 can significantly improve the spatial learning-memory ability of D-gal-induced aging rats.

Effect of EUK-134 on Body Weight and Brain Weight of D-Gal Treated Rats

D-gal group rats injected with D-gal (100mg/kg, s.c.) daily for six weeks experienced a statistically significant loss ($p < 0.05$) in body weight compared with normal group rats, while EUK-134 administration in D-gal+EUK-134 group or DPZ administration in D-gal+DPZ group reversed the animals' body weight loss (Figure 3A). Similarly, the brain weights of D-gal group rats significantly decreased compared with normal group rats, while EUK-134 administration in D-gal+EUK-134 group or DPZ administration in D-gal+DPZ group reversed the animals' brain weight loss (Figure 3B). Thus, it was indicated that administration of EUK-134 as well as DPZ can ameliorate the weight loss caused by the D-gal.

Effect of EUK-134 on Cerebral Cortex Thickness of D-Gal Treated Rats

D-gal group rats injected with D-gal (100mg/kg, s.c.) daily during six weeks experienced a statistically significant loss ($p < 0.01$) in cerebral cortex thickness compared with normal group rats, while EUK-134 administration in D-gal+EUK-134 group or DPZ administration in D-gal+DPZ group partly reversed the cerebral cortex loss (Table 1). In particular, administration of EUK-134 remarkably ameliorated the cerebral cortex loss caused by the D-gal.

Effect of EUK-134 on Pyramidal Neuron Density in Brain Hippocampus of D-Gal Treated Rats

We measured the pyramidal neuron density in CA1, CA2 and CA3 regions of brain hippocampus of four group rats on day 14, 28 and 42, and the results are shown in Table 2. The neuron densities in CA1, CA2

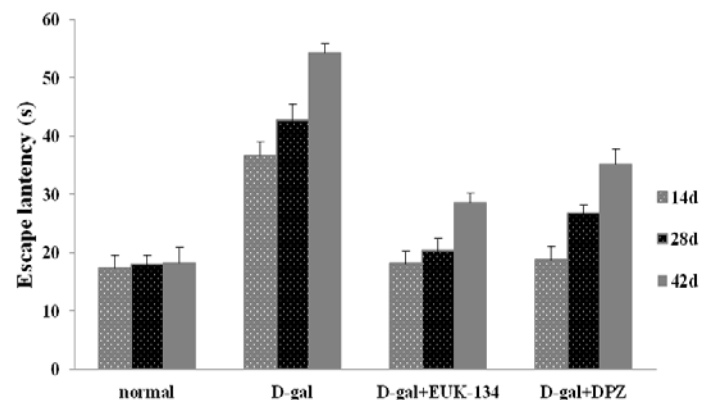


Figure 2: Effect of EUK-134 on the escape latencies of four group rats in the Morris water maze test on different days.

Values are expressed as the mean \pm SEM.

and CA1 of D-gal group rats all decreased significantly compared with those of normal group rats, and the longer the D-gal injection period, the less the neuron density. However, EUK-134 administration in D-gal+EUK-134 group or DPZ administration in D-gal+DPZ group significantly reversed the neuron density loss. Thus, administration of EUK-134 as well as DPZ could ameliorate the density loss caused by the D-gal.

Effect of EUK-134 on Pyramidal Layer Thickness in Brain Hippocampus of D-Gal Treated Rats

At the same time, we measured the pyramidal layer thickness in CA1, CA2 and CA3 regions of brain hippocampus of four group rats on day 14, 28 and 42, and the results are shown in Table 3. The layer thicknesses in CA1, CA2 and CA1 of D-gal group rats all decreased significantly compared with those of normal group rats, and the longer the D-gal

Table 1: Effect of EUK-134 on cerebral cortex thickness of rats treated with D-gal.

Group	Cerebral cortex thickness (μm)
Normal	1296 \pm 17
D-gal	988 \pm 16**
D-gal+EUK-134	1102 \pm 15* $\Delta\Delta$
D-gal+DPZ	1003 \pm 11* Δ

* $p < 0.05$, ** $p < 0.01$ (compared with normal group)

$\Delta p < 0.05$, $\Delta\Delta p < 0.01$ (compared with D-gal group)

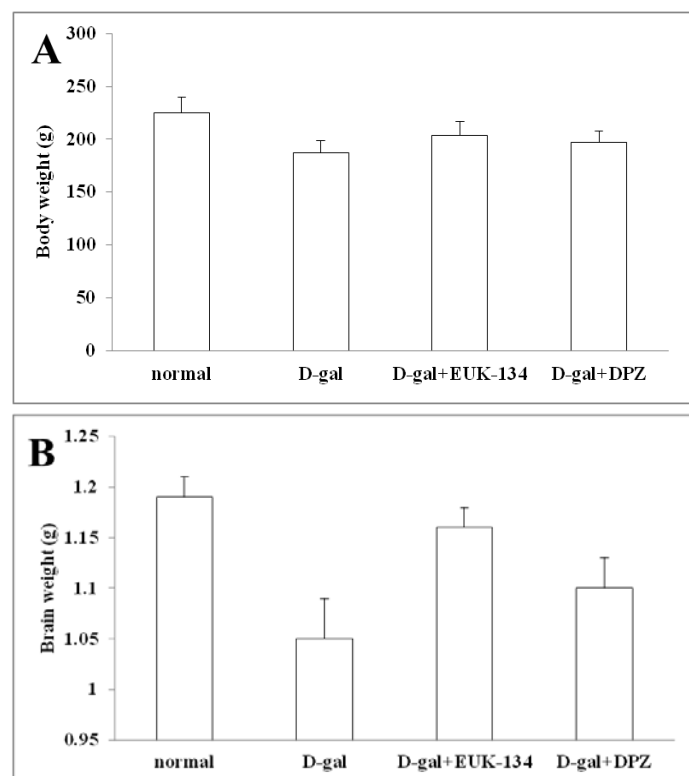


Figure 3: Effect of EUK-134 on (A) body weight and (B) brain weight of rats treated with D-gal.

injection period, the thinner the pyramidal layer. However, EUK-134 administration in D-gal+EUK-134 group or DPZ administration in D-gal+DPZ group significantly reversed the pyramidal layer loss. Thus, it was indicated that administration of EUK-134 as well as DPZ can ameliorate the layer loss caused by the D-gal.

Effect of EUK-134 on Some Biochemical Parameters of Oxidative Stress in Brain Tissues of D-Gal Treated Rats

The activities of SOD and CAT were all decreased in brain tissues of D-gal-induced aging rats, whereas EUK-134 administration or DPZ administration increased these antioxidant enzymes activities significantly (Figure 4A and Figure 4B). The levels of MDA, an index of lipid peroxide and oxidative stress, in the brain hippocampus and prefrontal cortex were increased markedly by the D-gal treatment and EUK-134 administration or DPZ administration resulted in less oxidative stress (Figure 4C). Interestingly, DPZ, which was not a SOD/CAT mimetic, as well as EUK-134, a SOD/CAT mimetic decreased oxidative stress, suggesting that the ameliorative effects of EUK-134

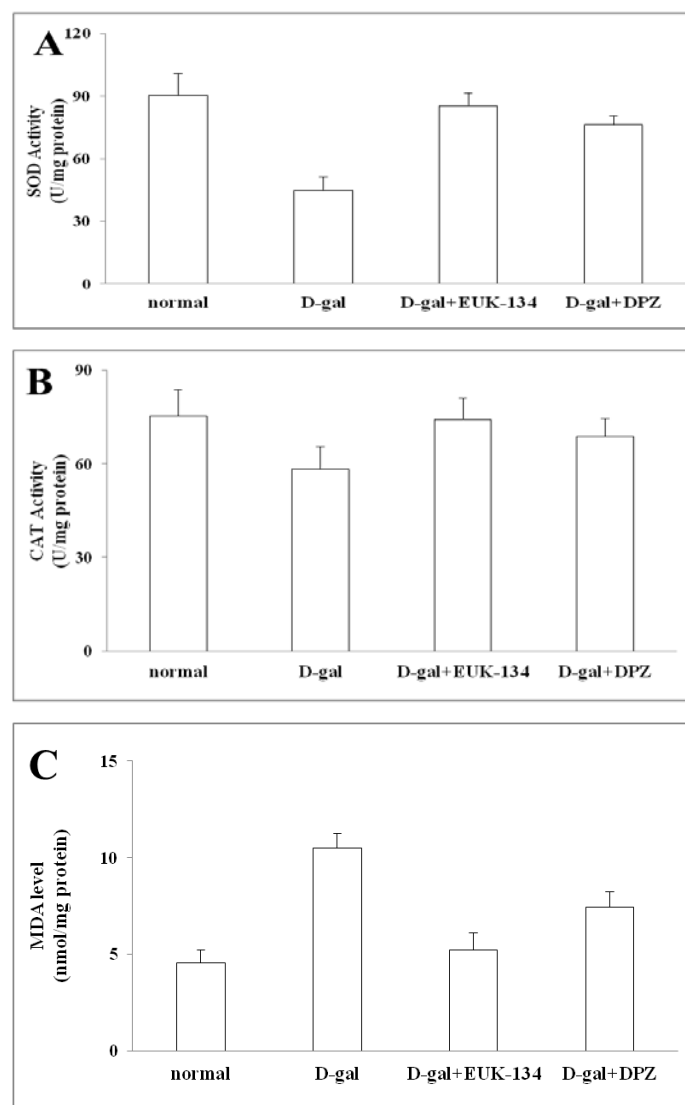


Figure 4: Effect of EUK-134 on (A) SOD activity, (B) CAT activity and (C) MDA level in brain tissues (the hippocampus and prefrontal cortex) of rats treated with D-gal.

Table 2: Effect of EUK-134 on pyramidal neuron density of rats treated with D-gal.

Regions of hippocampus	Day	Pyramidal neuron density (N/195×95µm ²)			
		Normal	D-gal	D-gal+EUK-134	D-gal+DPZ
CA1	14	21.0±2.2	18.1±2.8	19.3±1.4*	18.2±1.1*
	28	-	16.9±1.7	19.1±1.6* ^{△△}	18.5±1.1** [△]
	42	-	15.1±1.6*	19.3±1.8 ^{△△}	18.1±1.2* ^{△△}
CA2	14	24.4±1.7	20.9±1.6	16.7±1.3*	17.2±1.3**
	28	-	17.3±1.6**	18.7±2.6	17.7±1.3**
	42	-	15.9±1.2**	19.9±2.3 ^{△△}	18.0±1.2* ^{△△}
CA3	14	22.9±2.4	18.9±1.4	20.1±1.4	19.4±2.1**
	28	-	15.9±1.9**	20.1±1.6 ^{△△}	19.1±1.3** ^{△△}
	42	-	10.6±1.7**	21.4±1.6 ^{△△}	18.9±1.3** ^{△△}

*p<0.05, **p<0.01 (compared with normal group)

[△]p<0.05, ^{△△}p<0.01 (compared with D-gal group)**Table 3: Effect of EUK-134 on pyramidal layer thickness of rats treated with D-gal.**

Regions of hippocampus	Day	Pyramidal layer thickness (µm)			
		Normal	D-gal	D-gal+EUK-134	D-gal+DPZ
CA1	14	79.1±2.0	68.1±2.7**	72.1±2.9**	70.7±2.2*
	28	-	67.3±2.1**	77.7±2.5 ^{△△}	72.1±1.6** ^{△△}
	42	-	66.3±1.8**	78.8±2.7 ^{△△}	72.2±2.1** ^{△△}
CA2	14	86.3±2.7	80.1±2.9	80.1±2.5	80.2±1.3*
	28	-	77.1±2.3*	81.8±1.9 [△]	80.3±1.2* [△]
	42	-	71.9±2.9**	84.4±2.5 ^{△△}	81.3±1.1* ^{△△}
CA3	14	100.3±3.3	96.4±1.9*	97.2±2.1	97.1±1.1*
	28	-	90.1±2.8**	97.8±1.3* ^{△△}	97.2±2.1* ^{△△}
	42	-	86.8±2.6**	99.1±1.7 ^{△△}	97.3±1.2* ^{△△}

*p<0.05, **p<0.01 (compared with normal group)

[△]p<0.05, ^{△△}p<0.01 (compared with D-gal group)

and DPZ are associated with reduced oxidative stress and increased antioxidant enzymes activities in rats.

Effect of EUK-134 on AchE activity and Ach level in brain tissues of D-gal treated rats

AchE activity in the brain hippocampus and prefrontal cortex was increased in the D-gal treated rats compared with that of the normal group (Figure 5A), while the Ach level in the brain tissues was decreased in the D-gal treated rats compared with that of the normal group (Figure 5B).

DISCUSSION

D-gal, a kind of hexose, is an epimer of D-glucose, differing only in the configuration around C4. It rarely occurs free but is widely distributed in combined form in plants, animals, and microorganisms as a constituent of many oligo- and polysaccharides; it occurs also in galactolipids and is found almost exclusively in milk products as part of lactose (milk sugar). It is the major sugar obtained from hydrolysis of some marine biomass, such as red seaweed, and is also found in other food industrial sources such as cheese whey^[64] or molasses.^[65]

In the body of human beings and other mammals, D-Gal results from the hydrolysis of lactose by intestinal lactase to produce glucose and galactose. Two enzymes normally metabolize D-gal in the intestinal tract: galactokinase (GALK)^[66] and galactose-1-phosphate uridylyltransferase (GALT).^[67] At normal physiological concentrations, D-gal is metabolized through the evolutionarily conserved Leloir pathway.^[68,69] D-gal is first converted to galactose-1-phosphate by GALK, the second enzyme of the Leloir pathway. Then, galactose-1-phosphate reacts with UDP-glucose to produce UDP-galactose and glucose-1-phosphate via the action of GALT, the third enzyme of the Leloir pathway. Glucose-1-phosphate then enters the glycolytic pathway to generate energy, and UDP-galactose is converted back to UDP-glucose by UDP-galactose epimerase (GALE). However, accumulation of D-gal, due to its oversupply and its overwhelming the physiological metabolic capacity of the body, will lead to accumulation of toxic metabolites in the blocked Leloir pathway. For example, an overwhelming accumulation of galactose-1-phosphate potentially interferes with many important enzymes and is considered to be a major pathogenic agent for the organ (e.g., liver, brain and ovary)-specific toxicity exhibited by congenital GALT-deficiency (Type I) galactosaemia patients. On the other hand, excess D-gal leads

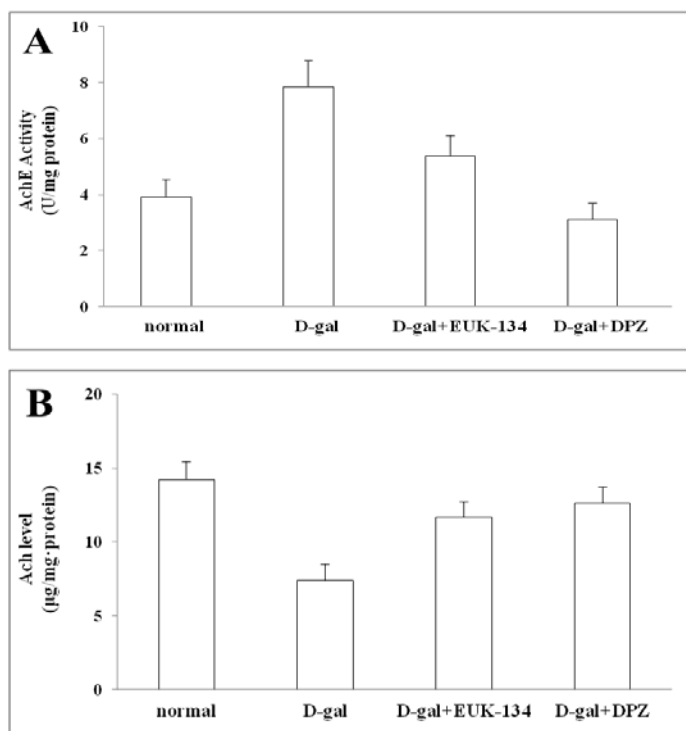


Figure 5: Effect of EUK-134 on (A) AChE activity and (B) Ach level in brain tissues (the hippocampus and prefrontal cortex) of rats treated with D-gal.

to the accumulation of galactitol, resulting in metabolic disorder, the accumulation of ROS and apoptosis.^[70]

In the present study, we utilized a rat model of oxidative stress and accelerated aging induced by chronic D-gal administration in order to study the availability of EUK-134, an SOD and CAT mimetic, in the prevention and treatment of neurodegenerative diseases such as AD.

First, we found through the the eight-arm radial maze test and the Morris water maze test that the administration of EUK-134 (5 mg/kg, i.a.) significantly improved the spatial memory of D-gal-induced aging rats, as did the administration of DPZ (1 mg/kg, oral). The aging of the brain is a cause of cognitive decline, specifically spatial memory decline in the elderly, which is frequently associated with AD, PD and other prevalent neurodegenerative diseases.^[71,72] One of the various symptoms experienced by patients with AD is trouble understanding visual images and spatial relationships.^[73,74] In addition, late stages of PD are associated with cognitive deficits, such as decreased attention, memory, and visuo-spatial functioning.^[75] Our results indicate that EUK-134 as well as DPZ can be used to ameliorate the age-related cognitive impairments which are becoming one of the most important issues for human health.

Second, we found through the weight measurement and the histopathological examination that the administration of EUK-134 (5 mg/kg, i.a.) significantly reversed the brain weight loss, the reduced cerebral cortex thickness, and the decreased pyramidal neuron density and the pyramidal layer in brain hippocampus of D-gal-induced aging rats, as did the administration of DPZ (1 mg/kg, oral). According to the previous data,^[76] changes in the brain that occur during aging process include cognitive deficits such as deterioration in spatial and associative memory, reduction in working memory and executive function and reduction in long-term potentiation and associated memory processes, physical characteristics changes such as reduction in overall brain mass, specifically hippocampus and prefrontal cortex, 30% reduction neurons in dorsolateral cortex and reduction of dendritic branching in superficial

cortical layers, physiological changes such as disruption in calcium receptor densities, increased amplitude of afterhyperpolarization and decrease in neuronal firing, cell-to-cell interactions such as loss of synapse connections in the hippocampal dentate gyrus, dysregulation of genes responsible for synapse protein synthesis and reduction of excitatory postsynaptic potentials and neuron cooperation, and genetic changes such as reduction of gene expression responsible for long-term potentiation, alterations in area CA1 of the hippocampus and reduced expression of genes responsible for synaptic plasticity. Some of those changes were reconfirmed in this study with regard to D-gal-induced aging and were efficiently prevented by the administration of EUK-134 as well as DPZ.

Finally, we found through the biochemical assays that the administration of EUK-134 (5 mg/kg, i.a.) significantly reversed the decreased SOD activity, the decreased CAT activity, the increased MDA level, the increased AChE activity and the decreased Ach level in the brain hippocampus and prefrontal cortex of D-gal-induced aging rats, as did the administration of DPZ (1 mg/kg, oral). As mentioned above, EUK-134 is a SOD/CAT mimetic but not an AChE inhibitor, while DPZ is not a SOD/CAT mimetic but an AChE inhibitor, thus indicating that the action mechanisms of two compounds may be different from each other though their effects are similar. This leads to future research extensions. It is well known the brain is especially sensitive to oxidative damage and possesses a relatively modest antioxidant defence.^[77,78] In the previous study^[79] as well as in this study, DPZ not only inhibited AChE activity but also increased antioxidant enzymes activity. Considering the fact that the D-gal induction decreased expressions of antioxidant enzyme genes including *Cat*, *Gpx1*, *Sod1* and *Sod2*,^[80] it is necessary in the future to investigate whether anti-oxidative effects of EUK-134 or DPZ in aged rats are associated with the expression of antioxidant enzyme genes. On the other hand, some researchers tested *in vivo* SOD activity of EUK compounds such as EUK-8 and EUK-134, which was done using a high-throughput SOD assay,^[81] with or without EDTA in the assay mixture in order to discriminate between endogenous SOD (not inhibited by EDTA) and SOD activity by EUK only (inhibited by EDTA). In addition, Michelle Keane and David Gems tested the *in vivo* effect of EUK-8 by evaluating the protective effect of EUK-8 in *Caenorhabditis elegans* upon administration of the superoxide generator paraquat.^[82] Using subcellular fractionation techniques, they have tested whether the SOD mimetics act at the most important cellular superoxide production site, i.e. the mitochondria. Using such techniques widely in the future will lead to clarification of precise molecular cell mechanisms of EUK-134's effect in the prevention and treatment of neurodegenerative diseases such as AD.

CONCLUSION

Findings of the present study indicate that EUK-134 possesses neuroprotective effects against D-galactose-induced senescence, probably due to its antioxidant enzyme activities and this shows the availability of EUK-134 in the prevention and treatment of neurodegenerative diseases such as Alzheimer's disease.

ACKNOWLEDGEMENT

This study was supported by the State Commission of Science and technology, DPR Korea.

CONFLICT OF INTEREST

The authors declare that they have no conflict of interest.

ABBREVIATIONS

ROS: Reactive Oxygen Species; **AD:** Alzheimer's Disease; **PD:** Parkinson's Disease; **D-gal:** D-galactose; **MDA:** Malondialdehyde; **SOD:** Superoxide Dismutase; **CAT:** Catalase; **DPZ:** Donepezil; **DW:** Distilled Water; **PBS:** Phosphate-Buffered Saline; **NBF:** Neutral Buffered Formalin; **H-E:** Hematoxylin-Eosin; **AchE:** Acetylcholine Esterase; **Ach:** Acetylcholine; **SEM:** Standard Error of Mean.

REFERENCES

- Booth LN, Brunet A. The aging epigenome. *Mol Cell*. 2016;62(5):728-44.
- Nadège KE, Agathe FL, Sylviane DNM, Carolle OA, Simon P, Antoine KK, et al. Antioxidant activities of *Dichrocephala integrifolia* (Linn.f.) O. Kuntze (Asteraceae) in a mice model of D-galactose-induced oxidative stress and accelerated aging. *Int J Pharmacol Phytochem Ethnomed*. 2017;8:41-53.
- Hof PR, Morrison JH. The aging brain: Morphomolecular senescence of cortical circuits. *Trends Neurosci*. 2004;27(10):607-13.
- Domínguez-González M, Puigpinós M, Jové M, Naudi A, Portero-Otín M, Pamplona R, et al. Regional vulnerability to lipoxidative damage and inflammation in normal human brain aging. *Exp Gerontol*. 2018;111:218-28.
- Nobakht-Haghighi N, Rahimifard M, Baeeri M, Rezvanfar MA, Nodeh SM, Haghi-Aminjan H, et al. Regulation of aging and oxidative stress pathways in aged pancreatic islets using alpha-lipoic acid. *Mol Cell Biochem*. 2018;449(1):267-76.
- Vina J, Borras C, Miquel J. Theories of aging. *IUBMB Life*. 2007;59(4-5):249-54.
- Perez VI, Bokov A, Remmen HV, Mele J, Ran Q, Ikeno Y, et al. Is the oxidative stress theory of aging dead?. *Biochim Biophys Acta*. 2009;1790(10):1005-14.
- Li Y. Antioxidants in biology and medicine: Essentials, advances, and clinical applications. New York: Nova Science Publishers; 2011;14-57.
- Jacobs HT. The mitochondrial theory of aging: Dead or alive?. *Aging Cell*. 2003;2(1):11-7.
- Brand MD, Nicholls DG. Assessing mitochondrial dysfunction in cells. *Biochem J*. 2011;435(2):297-312.
- Lin MT, Beal MF. Mitochondrial dysfunction and oxidative stress in neurodegenerative diseases. *Nature*. 2006;443(7113):787-95.
- Trushina E, McMurray CT. Oxidative stress and mitochondrial dysfunction in neurodegenerative diseases. *Neuroscience*. 2007;145(4):1233-48.
- Albers DS, Beal MF. Mitochondrial dysfunction and oxidative stress in aging and neurodegenerative disease. *J Neural Transm*. 2000;Suppl:59133-54.
- Anil K, Prakash A, Dogra S. Naringin alleviates cognitive impairment, mitochondrial dysfunction and oxidative stress induced by D-galactose in mice. *Food Chem Toxicol*. 2010;48(2):626-32.
- Patterson C. World Alzheimer Report 2018. Alzheimer's disease International. 2018. <https://www.alz.co.uk/research/world-report-2018>.
- Bonda DJ, Wang X, Lee HG, Smith MA, Perry G, Zhu X. Neuronal failure in Alzheimer's disease: A view through the oxidative stress looking-glass. *Neurosci Bull*. 2014;30(2):243-52.
- Zhang L, Zhao P, Yue C, Jin Z, Liu Q, Du X, et al. Sustained release of bioactive hydrogen by Pd hydride nanoparticles overcomes Alzheimer's disease. *Biomaterials*. 2019;197:393-404.
- Song X, Bao M, Li D, Li YM. Advanced glycation in D-galactose induced mouse aging model. *Mech Aging Dev*. 1999;108(3):239-51.
- Wei H, Li L, Song Q, Ai H, Chu J, Li W. Behavioural study of D-galactose induced aging model in C57BL/6J mice. *Behav Brain Res*. 2005;157(2):245-51.
- Zhang Q, Li X, Cui X, Zuo P. D-galactose injured neurogenesis in the hippocampus of adult mice. *Neurol Res*. 2005;27(5):552-6.
- Pourmemar E, Majdi A, Haramshahi M, Talebi M, Karimi P, Sadigh-Eteghad S. Intranasal cerebrolysin attenuates learning and memory impairments in D-galactose-induced senescence in mice. *Exp Gerontol*. 2017;87:16-22.
- Hacer TN, et al. Effect of *Capparis spinosa* L. on cognitive impairment induced by D-galactose in mice via inhibition of oxidative stress. *Turk J Med Sci*. 2015;45(5):1127-36.
- Yoo DY, et al. Melatonin improve D-galactose-induced aging effects on behavior, neurogenesis and lipid peroxidation in the mouse dentate gyrus via increasing pCREB expression. *J Pineal Res*. 2012;52(1):21-8.
- Ho SC, Liu JH, Wu RY. Establishment of the mimetic aging effect in mice caused by D-galactose. *Biogerontology*. 2003;4(1):15-8.
- Turgut NH, Mert DG, Kara H, Egilmez HR, Arslanbas E, Tepe B, et al. Effect of black mulberry (*Morus nigra*) extract treatment on cognitive impairment and oxidative stress status of D-galactose-induced aging mice. *Pharm Biol*. 2015;1-13.
- Zhang W, Bai M, Xi Y, Hao J, Liu L, Mao N, et al. Early memory deficits precede plaque deposition in APPswe/PS1dE9 mice: Involvement of oxidative stress and cholinergic dysfunction. *Free Radic Biol Med*. 2012;52(8):1443-52.
- Day BJ. Catalytic antioxidants: A radical approach to new therapeutics. *Drug Discov Today*. 2004;9(13):557-66.
- Iranzo O. Manganese complexes displaying superoxide dismutase activity: A balance between different factors: Minireview. *Bioorg Chem*. 2011;39(2):73-87.
- Ali B, Shakir MR, Iqbal MA. Techniques in the synthesis of mononuclear manganese complexes: A review. *Rev Inorg Chem*. 2017;1-26.
- Baudry M, Etienne S, Bruce A, Palucki M, Jacobsen E, Malfroy B. Salen-manganese complexes are superoxide dismutase-mimics. *Biochem Biophys Res Commun*. 1993;192(2):964-8.
- Gianello P, Saliez A, Bufkens X, Pettinger R, Misseley D, Hori S, et al. EUK-134, a synthetic superoxide dismutase and catalase mimetic, protects rat kidneys from ischemia-reperfusion-induced damage. *Transplantation*. 1996;62(11):1664-6.
- Doctrow SR, Huffman K, Marcus CB, Musleh W, Bruce A, Baudry M, et al. Salen-manganese complexes: Combined superoxide dismutase/catalase mimics with broad pharmacological efficacy. *Adv Pharmacol*. 1997;38:247-69.
- Melov S, Ravenscroft J, Malik S, Gill MS, Walker DW, Clayton PE, et al. Extension of life-span with superoxide dismutase/catalase mimetics. *Science*. 2000;289(5484):1567-9.
- Magwere T, West M, Riyahi K, Murphy MP, Smith RAJ, Partridge L. The effects of exogenous antioxidants on lifespan and oxidative stress resistance in *Drosophila melanogaster*. *Mech Aging Develop*. 2006;127(4):356-70.
- Doctrow SR, Liesa M, Melov S, Shirihai OS, Tofilon P. Salen Mn complexes are superoxide dismutase/catalase mimetics that protect the mitochondria. *Curr Inorg Chem*. 2012;2(3):325-34.
- Ma LL, Li Y, Yin PP, Kong FJ, Guo JJ, Shi HT, et al. Hypertrophied myocardium is vulnerable to ischemia/reperfusion injury and refractory to rapamycin-induced protection due to increased oxidative/nitritive stress. *Clin Sci*. 2018;132(1):93-110.
- Purushothaman S, Nair RR. Mitoprotective antioxidant EUK-134 stimulates fatty acid oxidation and prevents hypertrophy in H9C2 cells. *Mol Cell Biochem*. 2016;420(1):185-94. DOI:10.1007/s11010-016-2788-9.
- Kumar A, Shukla S, Chauhan AK, Singh D, Pandey HP, Singh C. The manganese-salen compound EUK-134 and N-acetyl cysteine rescue from zinc- and paraquat-induced toxicity in rat polymorphonuclear leukocytes. *Chem Biol Interact*. 2015;231:18-26.
- Himori K, Abe M, Tatebayashi D, Lee J, Westerblad H, Lanner JT, et al. Superoxide dismutase/catalase mimetic EUK-134 prevents diaphragm muscle weakness in monocrotaline-induced pulmonary hypertension. *PLoS One*. 2017;12(2):e0169146.
- Klein D, Steens J, Wiesemann A, Schulz F, Kaschani F, Röck K, et al. Mesenchymal stem cell therapy protects lungs from radiation-induced endothelial cell loss by restoring superoxide dismutase 1 expression. *Antioxid Redox Signal*. 2017;26(11):563-82.
- Magder S, Parthenis DG, AlGhoul I. Preservation of renal blood flow by the antioxidant EUK-134 in LPS-treated pigs. *Int J Mol Sci*. 2015;16(4):6801-17.
- Kamarehei M, Yazdanparast R. Modulation of Notch signaling pathway to prevent H₂O₂/menadione-induced SK-N-MC cells death by EUK134. *Cell Mol Neurobiol*. 2014;34(7):1037-45.
- SanMartin CD, Veloso P, Adasme T, Lobos P, Bruna B, Galaz J, et al. RyR2-Mediated Ca²⁺ Release and Mitochondrial ROS Generation Partake in the Synaptic Dysfunction Caused by Amyloid β Peptide Oligomers. *Front Mol Neurosci*. 2017;10(115):1-17.
- Sharpe MA, Olsson R, Stewart VC, Clark JB. Oxidation of nitric oxide by oxomanganese-salen complexes: A new mechanism for cellular protection by superoxide dismutase/catalase mimetics. *Biochem J*. 2002;366(Pt1):97-107.
- Boucher LJ. Manganese Schiff's base complexes II: Synthesis and spectroscopy of chloro-complexes of some derivatives of (salicylaldehydeethylenediimato) manganese (III). *J Inorg Nucl Chem*. 1974;36(3):531-6.
- Baker K, Marcus CB, Huffman K, Kruk H, Malfroy B, Doctrow SR. Synthetic combined superoxide dismutase/catalase mimetics are protective as a delayed treatment in a rat stroke model: A key role for reactive oxygen species in ischemic brain injury. *J Pharmacol Exp Ther*. 1998;284(1):215-21.
- Declercq L, Sente I, Hellemans L, Corstjens H, Maes D. Use of the synthetic superoxide dismutase/catalase mimetic EUK-134 to compensate for seasonal antioxidant deficiency by reducing pre-existing lipid peroxides at the human skin surface. *J Cosmetic Sci*. 2004;26(5):255-63.
- Doctrow SR, Huffman K, Marcus CB, Tocco G, Malfroy E, Adinolfi CA, et al. Salen-manganese complexes as catalytic scavengers of hydrogen peroxide and cytoprotective agents: Structure-activity relationship studies. *J Med Chem*. 2002;45(20):4549-58.
- Shindo T, Takasaki K, Uchida K, Onimura R, Kubota K, Uchida N, et al. Ameliorative effects of telmisartan on the inflammatory response and impaired spatial memory in a rat model of Alzheimer's disease incorporating additional cerebrovascular disease factors. *Biol Pharm Bull*. 2012;35(12):2141-7.
- Gocmez SS, Gacar N, Utkan T, Gacar G, Scarpaced PJ, Tumer N. Protective effects of resveratrol on aging-induced cognitive impairment in rats. *Neurobiol Learn Mem*. 2016;131:131-6.
- Zhang BX, Yin Y, Sun H, Ge H, Li W. Effects of sulforaphane and vitamin E on cognitive disorder and oxidative damage in lead-exposed mice hippocampus at lactation. *J Trace Elem Med Biol*. 2017;44:88-92.

52. Lu X, He S, Li Q, Yang H, Jiang X, Lin H, et al. Investigation of multi-target-directed ligands (MTDLs) with butyrylcholinesterase (BuChE) and indoleamine 2,3-dioxygenase 1 (IDO1) inhibition: The design, synthesis of miconazole analogues targeting Alzheimer's disease. *Bioorg Med Chem*. 2018;26(8):1665-74.
53. Glowinski J, Iversen LL. Regional studies of catecholamines in the rat brain. I. The disposition of [³H] norepinephrine, [³H] dopamine and [³H] dopa in various regions of the brain. *J Neurochem*. 1966;13(8):655-69.
54. Ibrahim WW, Abdelkader NF, Ismail HM, Khattab MM. Escitalopram ameliorates cognitive impairment in D-galactose-injected ovariectomized rats: Modulation of JNK, GSK-3 β , and ERK signaling pathways. *Scientific Reports*. 2019;9(1):10056.
55. Davies DC, Horwood N, Isaacs SL, Mann DM. The effect of age and Alzheimer's disease on pyramidal neuron density in the individual fields of the hippocampal formation. *Acta Neuropathol Berl*. 1992;83(5):510-7.
56. Oyanagui Y. Reevaluation of assay methods and establishment of kit for superoxide dismutase activity. *Anal Biochem*. 1984;142(2):290-6.
57. Ito Y, Nakachi K, Imai K, Hashimoto S, Watanabe Y, Inaba Y, et al. Stability of frozen serum levels of insulin-like growth factor-I, insulin-like growth factor-II, insulin-like growth factor binding protein-3, transforming growth factor β , soluble Fas, and superoxide dismutase activity for the JACC study. *J Epidemiol*. 2005;15(Suppl_1):S67-73.
58. Hadwan MH, Abed HN. Data supporting the spectrophotometric method for the estimation of catalase activity. *Data in Brief*. 2016;6:194-9.
59. Tsikas D. Assessment of lipid peroxidation by measuring malondialdehyde (MDA) and relatives in biological samples: Analytical and biological challenges. *Anal Biochem*. 2017;524:13-30.
60. Garcia YJ, Rodriguez-Malaver AJ, Penalzoa N. Lipid peroxidation measurement by thiobarbituric acid assay in rat cerebellar slices. *J Neurosci Methods*. 2005;144(1):127-35.
61. Perry M, Li Q, Kennedy RT. Review of recent advances in analytical techniques for the determination of neurotransmitters. *Anal Chim Acta*. 2009;653(1):1-22.
62. Zhou YZ, Zhao F-F, Gao L, Du G-H, Zhang X, Qin X-M. Licorice extract attenuates brain aging of D-galactose induced rats through inhibition of oxidative stress and attenuation of neuronal apoptosis. *RSC Adv*. 2017;7(75):47758-66.
63. Zhang C, Xia Y, Jiang W, Wang C, Han B, Hao J. Determination of non-neuronal acetylcholine in human peripheral blood mononuclear cells by use of hydrophilic interaction ultra-performance liquid chromatography-tandem Mass spectrometry. *J Chromatogr B*. 2016;1022:265-73.
64. Siso M. The biotechnological utilization of cheese whey: A review. *Bioresour Technol*. 1996;57(1):1-11.
65. Fischer K, Bipp HP. Generation of organic acids and monosaccharides by hydrolytic and oxidative transformation of food processing residues. *Bioresour Technol*. 2005;96(7):831-42.
66. Keenan T, Mills R, Pocock E, Budhadev D, Parmeggiani F, Flitsch S, et al. The characterisation of a galactokinase from *Streptomyces coelicolor*. *Carbohydr Res*. 2019;472:132-7.
67. Benini S, Toccafondi M, Rejzek M, Musiani F, Wagsta BA, Wuerges J, et al. Glucose-1-phosphate uridylyltransferase from *Erwinia amylovora*: Activity, structure and substrate specificity. *BBA-Proteins Proteom*. 2017;1865(11):1348-57.
68. Frey PA. The Leloir pathway: A mechanistic imperative for three enzymes to change the stereochemical configuration of a single carbon in galactose. *FASEB J*. 1996;10(4):461-70.
69. Holden HM, Rayment I, Thoden JB. Structure and function of enzymes of the Leloir pathway for galactose metabolism. *J Biol Chem*. 2003;278(45):43885-8.
70. Lai K, Elsas LJ, Wierenga KJ. Galactose toxicity in animals. *IUBMB Life*. 2009;61(11):1063-74.
71. Yankner BA, Lu T, Loerch P. The aging brain. *Annu Rev Pathol*. 2008;3:41-66.
72. Bishop NA, Lu T, Yankner BA. Neural mechanisms of aging and cognitive decline. *Nature*. 2010;464(7288):529-35.
73. Alzheimer's Association. 10 early signs and symptoms of Alzheimer's. 2012. Retrieved from http://www.alz.org/alzheimers_disease_10_signs_of_alzheimers.asp.
74. Boyle PA, Yang J, Yu L, Leurgans SE, Capuano AW, Schneider JA, et al. Varied effects of age-related neuropathologies on the trajectory of late life cognitive decline. *Brain*. 2017;140(3):804-12.
75. Emre M, Aarsland D, Brown R, Burn DJ, Duyckaerts C, Mizuno Y, et al. Clinical diagnostic criteria for dementia associated with Parkinson's disease. *Mov Disord*. 2007;22(12):1689-707.
76. Wahl D, Cogger VC, Solon-Biet SM, Waern RVR, Gokarn R, Pulpitel T, et al. Nutritional strategies to optimize cognitive function in the aging brain. *Aging Res Rev*. 2016;31:80-92.
77. Halliwell B. Oxidative stress and neurodegeneration: Where are we now?. *J Neurochem*. 2006;97(6):1634-58.
78. Ng F, Berk M, Dean O, Bush AI. Oxidative stress in psychiatric disorders: evidence base and therapeutic implications. *Int J Neuropsychopharmacol*. 2008;11(6):1-26.
79. Ghumatkar PJ, Patil SP, Jain PD, Tambe RM, Sathaye S. Nootropic, neuroprotective and neurotrophic effects of phloretin in scopolamine induced amnesia in mice. *Pharmacol Biochem Be*. 2015;135:182-91. doi:10.1016/j.pbb.2015.06.005.
80. Ni Y, Wu T, Yang L, Xu Y, Ota T, Fu Z. Protective effects of astaxanthin on a combination of D-galactose and jet lag-induced aging model in mice. *Endocr J*. 2018;65(5):569-78.
81. Lenaerts I, Braeckman BP, Matthijssens F, Vanfleteren JR. A high-throughput microtiter plate assay for superoxide dismutase based on lucigenin chemiluminescence. *Anal Biochem*. 2002;311(1):90-2.
82. Keaney M, Gems D. No increase in lifespan in *Caenorhabditis elegans* upon treatment with the superoxide dismutase mimetic EUK-8. *Free Radic Biol Med*. 2003;34(2):277-82.
83. Figure 3: Effect of EUK-134 on (A) body weight and (B) brain weight of rats treated with D-gal.

Cite this article: Kim KW, Kim KS, Ri KO, Ri HG, Yo CI, Ko SY, et al. Ameliorative Effects of EUK-134, a Superoxide Dismutase and Catalase Mimetic, in a Rat Model of D-Galactose-Induced Oxidative Stress and Accelerated Aging. *Int J Clin Exp Physiol*. 2022;9(1):19-27.